Talanta 93 (2012) 79–85

Contents lists available at SciVerse ScienceDirect

Talanta

journal homepage: www.elsevier.com/locate/talanta

Simultaneous determination of L-ascorbic acid, dopamine and uric acid with gold nanoparticles–β-cyclodextrin–graphene-modified electrode by square wave voltammetry

Xianqing Tian[a], Changming Cheng[b], Hongyan Yuan[b], Juan Du[a], Dan Xiao[a,b,*], Shunping Xie[c], Martin M.F. Choi[c,**,1]

[a] College of Chemistry, Sichuan University, 29 Wangjiang Road, Chengdu 610064, PR China
[b] College of Chemical Engineering, Sichuan University, 29 Wangjiang Road, Chengdu 610065, PR China
[c] Department of Chemistry, Hong Kong Baptist University, 224 Waterloo Road, Kowloon Tong, Hong Kong SAR, PR China

ARTICLE INFO

Article history:
Received 5 November 2011
Received in revised form 20 January 2012
Accepted 29 January 2012
Available online 2 February 2012

Keywords:
Graphene
β-Cyclodextrin
Electroanalysis
L-Ascorbic acid
Dopamine
Uric acid

ABSTRACT

Graphene decorated with gold nanoparticles (AuNPs–β-CD–Gra) has been synthesized by *in situ* thermal reduction of graphene oxide and $HAuCl_4$ with β-cyclodextrin (β-CD) under alkaline condition. The AuNPs–β-CD–Gra product was well characterized by infrared spectroscopy, X-ray powder diffraction, scanning electron microscopy, high-resolution transmission electron microscopy, and selected area electron diffraction. This material was used to fabricate an AuNPs–β-CD–Gra-modified glassy carbon electrode (GCE) which showed excellent electro-oxidation of L-ascorbic acid (AA), dopamine (DA) and uric acid (UA) in 0.10 M NaH_2PO_4–HCl buffer solution (pH 2.0) by square wave voltammetry (SWV). Three well-resolved oxidation peaks of AA and DA and UA were obtained. The AuNPs–β-CD–Gra/GCE exhibits linear responses to AA, DA and UA in the ranges 30–2000, 0.5–150 and 0.5–60 μM, respectively. The detection limits (based on $S/N = 3$ and preconcentration time = 3.0 min) for AA, DA and UA are 10, 0.15 and 0.21 μM, respectively. The AuNPs–β-CD–Gra/GCE has been successfully applied to determine UA in human urine with satisfactory results. Our work provides a simple, convenient and green route to synthesize AuNPs on Gra which is potentially useful in electroanalysis.

Introduction

Nanomaterials have shown unique and special properties that are differ from the bulk materials, originating from their quantum-scale dimensions [1]. So far gold [2–4], silver [5,6], platinum [7,8], and palladium [9] nanomaterials have attracted considerable interests and studies in the past two decades. Among these, gold nanomaterials have been successfully applied to fabricate various types of optical [10,11], electrochemical [12,13] sensors and biosensors [14], owning to their good conductivity, electrocatalytic ability, and biocompatibility. To our knowledge, a lot of useful materials like polymer [4,15], carbon nanotubes [13,16–18], graphene oxide (GO) and/or graphene (Gra) [19–31] have been used as substrates to assemble gold nanomaterials. In many of the developed assemble strategies of gold nanomaterials, GO or Gra has received much attention, attributing to its specific nanostructure and ability to enhance the performance of nanocomposites. Tuan et al. [19] immobilized gold nanoparticles (AuNPs) on GO sheet *via* an amidation reaction. Mao et al. [23] directly assembled AuNPs-antibody conjugates on thermally reduced GO sheet to form a field-effect transistor biosensor which shows high sensitivity and selectivity to specific proteins. Muszynski et al. [24] explored a solution-based approach to anchor AuNPs on octadecylamine functionalized Gra and the hybrid material is very useful for surface plasmon application. Liu et al. [31] developed a co-electrodeposition route to synthesize Gra–Au nanocomposite which shows potential application for electroanalysis. Malola et al. [22] used density-functional theory to confirm that AuNPs could be in-plane adsorbed on Gra. Since this AuNPs–Gra hybrid material exhibits favorable electrochemical properties, it is worth to explore its applications in various fields.

L-Ascorbic acid (AA), a soluble vitamin, is an essential nutrient for humans. In living organisms, AA is an antioxidant which can protect the body against oxidative stress [32]. Dopamine (DA) is a catecholamine neurotransmitter which plays an important physiological role as an extracellular chemical messenger. Uric

* Corresponding author at: College of Chemistry, Sichuan University, 29 Wangjiang Road, Chengdu 610064, PR China. Tel.: +86 28 85416029; fax: +86 28 85415029.
** Corresponding author.
E-mail addresses: xiaodan@scu.edu.cn (D. Xiao), mfchoi@hkbu.edu.hk (M.M.F. Choi).
[1] Tel.: +852 34117839; fax: +852 34117348.

0039-9140/$ – see front matter © 2012 Elsevier B.V. All rights reserved.
doi:10.1016/j.talanta.2012.01.047

acid (UA) is a relatively water-insoluble end product of purine metabolism in humans and is excreted *via* urine. UA also coexists with AA and DA in biological fluids such as blood and urine. An abnormally high level of UA (DA and/or AA) is usually a symptom of illness. Therefore, simultaneous determination of these compounds is of particular importance [33]. Since these compounds show voltammetric responses on traditional bare electrodes (*e.g.*, glassy carbon electrode) at very close working potentials, it is rather difficult to simultaneously determine their contents in biological samples without sample pretreatment [34]. Various active materials including polymers [6,8,35–42], noble metal/alloy nanoparticles (NPs) [6,8,43–45], oxides [46,47], and carbon-based materials [9,41,48–54] have been applied to simultaneously determine AA, DA and UA with moderate success. Recently Han et al. [53] used a chitosan-Gra modified electrode to well resolve the oxidation potentials of AA, DA and UA. Similarly, Liu et al. [31] demonstrated that Gra–Au nanocomposite is a promising material for simultaneous electroanalysis of AA, DA and UA. As such, to move forward, we incorporated both AuNPs and β-cyclodextrin (β-CD) on Gra to fabricate a modified glassy carbon electrode (GCE). The AuNPs–β-CD–Gra/GCE shows better analytical performance for simultaneous determination of AA, DA and UA.

In this work, we propose a simple green one-pot synthesis of AuNPs on Gra by *in situ* thermal reduction of hydrogen tetrachloroaurate(III) ($HAuCl_4$) and GO with β-CD in alkaline condition. During the synthesis process, β-CD on Gra sheet not only acts as dispersant and stabilizer for $HAuCl_4$ but also serves as a reducing agent to reduce GO and $AuCl_4^-$ to Gra and AuNPs, respectively. The resulting AuNPs–β-CD–Gra composite can be easily purified, stored and redispersed in water without any further chemical treatment. Finally, the GCE modified with AuNPs–β-CD–Gra has been used to simultaneously determine AA, DA and UA by square wave voltammetry (SWV). Additionally, it has been successfully applied to determine the UA content in human urine with satisfactory results. Our work demonstrates that the developed AuNPs–β-CD–Gra/GCE shows potential in biomedical or clinical analysis.

Experimental

Chemicals and reagents

Graphene oxide was purchased from ACS Material (Warwick, RI, USA). L-Ascorbic acid, β-cyclodextrin, dopamine, hydrochloric acid (HCl), hydrogen tetrachloroaurate(III), sodium dihydrogen phosphate dihydrate ($NaH_2PO_4{\cdot}2H_2O$), sodium hydroxide (NaOH), and uric acid were obtained from Sigma–Aldrich (St. Louis, MO, USA). All chemicals of analytical reagent grade or above were used as received without further purification. Buffer solutions were prepared from $NaH_2PO_4{\cdot}2H_2O$ and HCl in the pH range 1.0–5.0. Freshly prepared solutions of AA, DA and UA were used in all experiments. Double distilled water (DDW) was used throughout the work.

Instrumentation

Scanning electron microscopic (SEM) images were obtained from a Hitachi S4800 SEM (Tokyo, Japan). High-resolution transmission electron microscopic (HRTEM) image and selected area electron diffraction (SAED) pattern were acquired on a FEI Tecnai G^2 20 HRTEM (Hillsboro, OR, USA). X-ray powder diffraction (XRD) was conducted on a TD-3500 XRD (Tongda Instrument Co., Dandong, China) with Cu Kα radiation source. Infrared (IR) spectra were collected on a Thermo Scientific Nicolet 6700 Fourier transform IR spectrometer (Sugar Land, TX, USA). The pH measurements were taken on a Thermo Origin 720A+ pH/ion meter (Thermo Electron Corporation, Waltham, MA, USA).

Preparation of AuNPs–β-CD–Gra composite

The preparation of Gra [55] and synthesis of AuNPs through β-CD reduction [56] were based on literature methods with modifications to a one-pot synthesis. In essence, GO, β-CD and $HAuCl_4$ were mixed and heated in an alkaline solution at 60 °C for 2 h. The reaction mixture was then subject to centrifugation, cleansed with DDW and finally vacuum dried to obtain the AuNPs–β-CD–Gra product. The reaction mechanisms are illustrated in Scheme 1 and the preparation details are deposited in Supplementary data. For comparison, AuNPs–Gra, Gra–β-CD and AuNPs–β-CD composites were also prepared in similar procedures.

Fabrication of AuNPs–β-CD–Gra modified electrode

A homogeneous dispersion of AuNPs–β-CD–Gra aqueous solution was prepared by sonication of 1.0 mg AuNPs–β-CD–Gra composite in 1.0 mL DDW for 30 min. Before electrode modification, a GCE (3.0 mm diameter) was polished with 0.1, 0.3 and 0.05 μm Al_2O_3 slurry sequentially to mirror-like smoothness, rinsed with DDW, and followed by sonication in nitric acid solution (1:1 v/v), absolute ethanol and DDW. Then the clean GC electrode was immersed in a 0.50 M H_2SO_4 and cyclic voltammetry (CV) from −0.20 to +0.80 V for 20 cycles at 50 mV/s were performed. These CV scans aid to remove any impurities/residues and also introduce some active functional groups such as —COOH or —OH on the freshly polished glassy carbon electrode. This typical electrochemical polish procedure permits GCE to have more reproducible and well-defined electrochemical behavior. Afterwards, the GC was rinsed with DDW and dried with a stream of nitrogen (N_2), an aliquot of 5.0 μL AuNPs–β-CD–Gra aqueous solution was dropped onto the surface of the GCE and dried under an IR lamp for 1 h to obtain the AuNPs–β-CD–Gra modified GCE (AuNPs–β-CD–Gra/GCE). In the control experiments, 5.0 μL of 1.0 mg/mL Gra–β-CD suspension, AuNPs–β-CD and β-CD solution were also cast onto bare GCEs to obtain the Gra–β-CD/GCE, AuNPs–β-CD/GCE and β-CD/GCE, respectively.

Electrochemical measurement

All electrochemical measurements were performed on a Lanlike LK2006 electrochemical workstation (Tianjin, China). The conventional three-electrode system, comprising a bare or modified GCE as the working electrode, a saturated calomel electrode (SCE) as the reference electrode and a platinum foil as the counter electrode, was used. A single compartment electrochemical cell at ambient conditions was used throughout the work. The solutions were deoxygenated with a stream of high purity N_2 (99.99%) at least

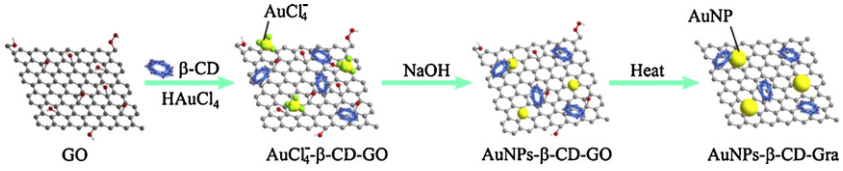

Scheme 1. Schematic illustrates the reaction steps of AuNPs–β-CD–Gra.

10 min prior to each electrochemical measurement and blanketed under N_2 atmosphere to keep oxygen from the solutions. Known concentrations of AA, DA and UA standards were spiked into the cell. Preconcentration of analytes on the modified GCE at open circuit potential (OCP) under constant stirring was conducted. After a specific time, CV or SWV at various scan rates was performed in quiescent solution. The SWVs were recorded by applying a positive-going SWV potential scan (0.00–0.70 V) under optimal conditions: step potential 1 mV, frequency 15 Hz and amplitude 40 mV.

Sample analysis

Known standard mixtures of AA, DA and UA were injected into the electrolyte and analyzed under the optimal SWV conditions. The voltammetric peak currents of AA, DA and UA were recorded and used for constructing calibration curves. Human urine samples were supplied by a local hospital. Without any sample pretreatment, an aliquot of 50 μL human urine was directly added into the electrolyte and analyzed by SWV. The peak currents of the analytes were recorded and their concentrations were determined. Recovery tests were conducted by adding known amounts of AA, DA and UA to the urine samples and followed with the same SWV analysis. All sample analyses were repeated three times.

Results and discussion

Preparation of AuNPs on graphene

Stable Gra suspension could be quickly prepared in strong alkaline condition through heating under moderate temperatures [55]. It has been reported that β-CD could reduce some metals (gold and silver) or alloy to NPs under strong alkaline condition [56]. As such, an alkaline β-CD solution was used to prepare our Gra–AuNPs hybrid material. Scheme 1 illustrates the synthetic mechanisms of AuNPs–β-CD–Gra composite. β-CD and $HAuCl_4$ were added to a GO suspension to promote the interaction of Au(III) complex and β-CD with oxygen moiety on the GO surface [57]. Fig. 1S (Supplementary data) displays the optical images of the reaction mixtures with different concentrations of $HAuCl_4$. GO was deoxygenated to Gra by OH^- [55] while Au(III) complex was reduced to AuNPs by β-CD [56]. When a higher concentration of $HAuCl_4$ is used, more AuNPs are formed and the solution turns to light purple (Fig. 1Sd). In essence, our proposed one-pot synthesis affords the growth of AuNPs on Gra by using alkaline β-CD at moderate temperature.

Characterization of AuNPs–β-CD–Gra composite

The as-prepared AuNPs–β-CD–Gra composite was fully characterized by XRD, IR, SEM, HRTEM, and SAED. The XRD patterns and IR spectra of β-CD, GO, β-CD–Gra, and AuNPs–β-CD–Gra are displayed in Figs. S2 and S3. The results indicate the presence of β-CD on Gra and the complete reduction of GO to Gra of the AuNPs–β-CD–Gra sample [53]. The detailed interpretation of the IR spectra and XRD patterns can be found in Supplementary Data. The morphology of the as-prepared AuNPs–β-CD–Gra was studied by SEM and depicted in Fig. 1A. The AuNPs–β-CD–Gra contains about 125 × 400–500 nm of nanosheets and the top right inset displays the magnified view of the nanosheets. It clearly shows the ribbon-like Gra sheets but AuNPs are difficult to observe. However, white dots (NPs) were clearly seen on the Gra nanosheets when the image was further magnified as shown in the bottom left inset. In order to confirm the identity of these NPs, HRTEM image and SAED pattern were captured and depicted in Fig. 1B and C, respectively. The SAED pattern was assigned to the diffraction from the (1 1 1), (2 2 0), (2 0 0) and (3 1 1) planes of the face-centered cubic gold crystal which is consistent with the JCPDS card no. 5-8601. The HRTEM shows the 0.23 nm inter-planar spacing of the AuNPs, indicating that the (1 1 1) crystal plane of the AuNP orientates on the Gra sheet. The AuNP is about 17 nm in diameter which is larger than that of the literature [56], possibly due to the long reaction time. These results confirm the successful synthesis of AuNPs on Gra sheets by *in situ* β-CD reduction and the as-prepared AuNPs–β-CD–Gra can be applied to electroanalysis (*infra vide*).

CV and SWV studies of AA, DA and UA at AuNPs–β-CD–Gra/GCE

Fig. 2 depicts the CV responses of AA, DA and UA at AuNPs–β-CD–Gra/GCE under various scan rates. The plots of the redox peak current as function of the square root of scan rates are shown in the insets of Fig. 2.

In all cases good linear relationships were observed, indicating that all these compounds are electro-active under diffusion-controlled processes at the AuNPs–β-CD–Gra/GCE. Fig. 2 shows that AA and UA are irreversibly electro-oxidized while DA displays a quasi-reversible response at the AuNPs–β-CD–Gra/GCE. The $\Delta E_p = |E_{pa} - E_{pc}|$ is 111 mV for DA at 50 mV/s. The anodic and cathodic peak potentials of DA at various scan rates are summarized in Table S1. The electro-oxidation of DA fits the case VII (*i.e.*, catalytic reaction with reversible charge transfer) based on the Nicholson and Shain criteria (Fig. S4) [58]. The electro-oxidation mechanisms of AA, DA and UA at AuNPs–β-CD/GCE are illustrated in Scheme 2.

Although AuNPs–β-CD–Gra/GCE responds well to AA, DA and UA, the oxidation potentials for these analytes are so close that it is difficult to accurately quantify them. Fortunately, when they are analyzed by SWV (*infra vide*), their oxidation peaks are much better resolved and the background current is lower (Fig. S5), allowing their simultaneous determination.

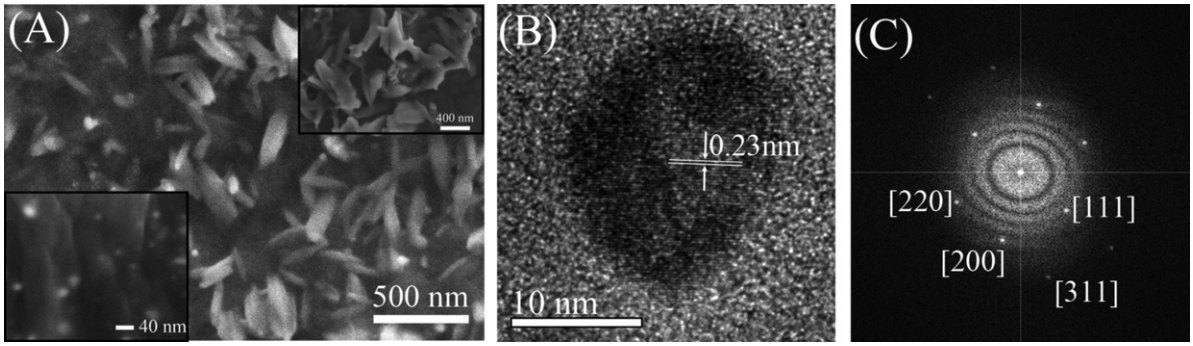

Fig. 1. (A) SEM image of AuNPs–β-CD–Gra on an aluminum substrate. Top right inset displays the SEM image of β-CD–Gra and bottom left inset shows the SEM image of AuNPs–β-CD–Gra at a higher magnification. (B) HRTEM image and (C) SAED pattern of AuNPs in the AuNPs–β-CD–Gra composite.

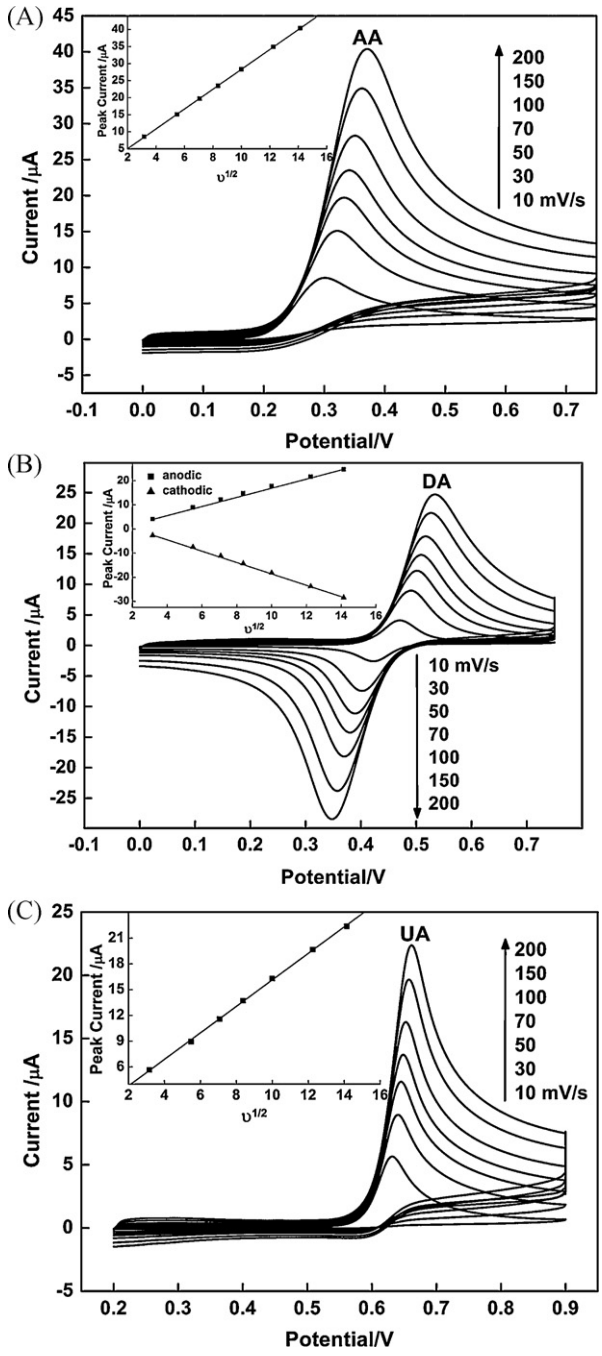

Fig. 2. CVs of (A) 1.0 mM AA, (B) 25 μM DA and (C) 25 μM UA in 0.10 M NaH_2PO_4–HCl buffer solution (pH 2.0) at AuNPs–β-CD–Gra/GCE at different scan rates (10–200 mV/s). The insets display the plots of peak current against square root of scan rate.

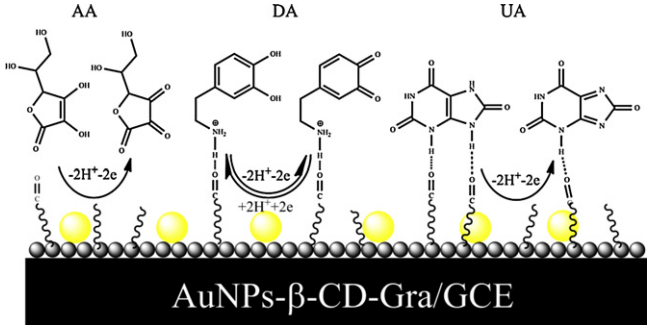

Scheme 2. The electro-oxidation of AA, DA and UA at AuNPs–β-CD-Gra/GCE.

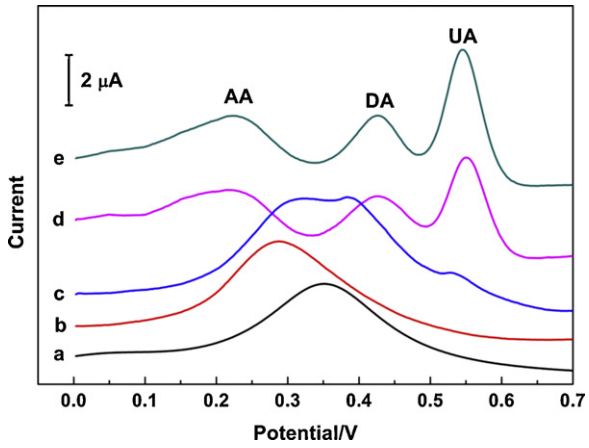

Fig. 3. SWVs of 500 μM AA, 15 μM DA and 15 μM UA in 0.10 M NaH_2PO_4–HCl buffer solution (pH 2.0) at different electrodes: (a) bare GCE, (b) β-CD/GCE, (c) AuNPs–β-CD/GCE, (d) β-CD–Gra/GCE and (e) AuNPs–β-CD–Gra/GCE. Square wave frequency: 15 Hz, amplitude: 40 mV and step potential: 1 mV, preconcentration time: 3.0 min.

Fig. 3 shows the SWV of AA, DA and UA at the AuNPs–β-CD–Gra/GCE. For comparison, bare GCE, β-CD/GCE, β-CD–Gra/GCE and AuNPs–β-CD/GCE were also studied. For the bare GCE, a rather broad oxidation peak at 0.352 V is observed which is derived from the simultaneous oxidation of AA, DA and UA [34]; unfortunately, the individual AA, DA and UA cannot be distinguished (Fig. 3a). Similarly, SWV of these analytes on β-CD/GCE or AuNPs–β-CD/GCE cannot resolve the individual compound (Fig. 3b and c).β-CD induces a slightly negative shift of the broad oxidation peak, inferring that AA, DA and UA are oxidized at lower working potential than that on bare GCE. AuNPs–β-CD can slightly resolve these analytes but the sensitivity is lower. The oxidation peaks for AA, DA and UA are better resolved at the β-CD–Gra/GCE (Fig. 3d) and AuNPs–β-CD-Gra/GCE (Fig. 3e), indicating that the presence of Gra on GCE indeed improves the resolution of these compounds. The oxidation potentials for AA, DA and UA are 0.222, 0.426 and 0.546 V, respectively, and the peak-to-peak separations (ΔE_p) of AA–DA and DA-UA are 204 and 120 mV, respectively. AuNPs on the β-CD–Gra/GCE do not shift the oxidation potential of these analytes but it can lower the background current and increase the oxidation currents by 3.0%, 13.8% and 35.4% for AA, DA and UA, respectively. These results obviously demonstrate that AuNPs can enhance the oxidation of DA and UA on the β-CD–Gra/GCE. Furthermore, the stability and reproducibility of the AuNPs–β-CD–Gra/GCE were examined by evaluating the SWV currents of 500 μM AA, 15 μM DA and 15 μM UA at this electrode. The RSDs ($n = 7$) were 0.3%, 1.7% and 1.9% for AA, DA and UA, respectively, indicating that the results are highly reproducible. This work and the findings lay a solid foundation for simultaneous determination of AA, DA and UA in real sample which will be discussed in the later section.

Effect of $HAuCl_4$ concentration on AuNPs–β-CD–Gra/GCE for SWV

It has been determined that AuNPs at AuNPs-β-CD-Gra/GCE can increase its SWV response to AA, DA and UA. In addition, the formation of AuNPs was mainly governed by the oxygen functionality on the surface of GO [57]. Thus it is essential to optimize the amount of $HAuCl_4$ for the synthesis of AuNPs–β-CD–Gra. Various AuNPs at AuNPs–β-CD–Gra/GCE were prepared from different concentrations of $HAuCl_4$. Fig. S6A displays the SWV peak currents of these modified electrodes against the concentration of $HAuCl_4$. It was determined that 0.050 mM $HAuCl_4$ produced the best response to

AA, DA and UA; and was thus chosen as the optimal concentration of $HAuCl_4$ for synthesis of AuNPs–β-CD–Gra hybrid material.

Effect of pH

In most cases, the electrolyte pH is an important parameter to the electrochemical reaction. Fig. S6B and C displays the effect of pH on the anodic peak potentials (E_{pa}) and current responses of AA, DA and UA at AuNPs–β-CD–Gra/GCE in 0.10 M NaH_2PO_4–HCl buffer solution. The anodic peak potentials for AA, DA and UA shift negatively with the increase in pH (1.0–5.0). The linear regression equations are $E_{pa} = -0.0567$ pH + 0.400 ($r = 0.991$) for AA, $E_{pa} = -0.0470$ pH + 0.0580 ($r = 0.999$) for DA and $E_{pa} = -0.0479$ pH + 0.689 ($r = 0.999$) for UA, demonstrating that the electrochemical reaction is a two-proton and a two-electron transfer process [33,59]. The peak currents of AA and DA do not change much at different pHs. However, for UA, the current decreases with the increase in pH (1.0–4.0) and then increases slightly at pH 5.0. The background current increases with the acidity of the buffer solution and the anodic peaks of DA and UA cannot be completely separated. Hence, pH 2.0 was chosen in this work.

Effect of preconcentration time

Fig. S6D depicts the effect of preconcentration time at OCP on the peak currents of AA, DA and UA. The currents increase with the increase in the preconcentration time, attributing to the adsorption of these analytes on the AuNPs–β-CD–Gra *via* hydrogen bonding between the carbonyl functionalities of the oxidized form of β-CD and analytes [56]. These results are consistent to that of AuNPs modified with over-oxidized polypyrrole for determination of epinephrine and UA [43]. For AA, the current increases slightly with a 3.1% enhancement for the first 1.0 min and then reaches the plateau for further increase in time. For DA and UA, the currents increase dramatically for the first 1.0 min and then level off gradually as the time increases. The enhancements in current for DA and UA are 57.5% and 114% at 3.0 min of preconcentration. Although the current response for UA continues to increase slightly after 3.0 min, the increase is very small. As such, 3.0 min was chosen as the optimal preconcentration time for AA, DA and UA in our subsequent work.

Effect of square wave frequency and amplitude

For SWV analysis, the square wave frequency not only affects the analysis time but also influences the peak potential and current. Fig. S6E depicts the current responses for AA, DA and UA against the square wave frequency. 15 Hz was chosen as the working square wave frequency because it produces the highest currents for both DA and UA and is only −12.0% to that at 25 Hz for AA. In addition, it is essential to choose an optimum square wave amplitude in order to obtain the highest peak current and minimize background current. Fig. S6F displays the SWV of AA, DA and UA at various square wave amplitudes. 40 mV was chosen as the optimal square wave amplitude for most of our work since it produces the highest peak currents and the peaks are well resolved.

Simultaneous determination of AA, DA and UA

The determination of AA, DA and UA at AuNPs–β-CD–Gra/GCE was performed under the optimal SWV conditions. Fig. 4A shows the SWVs of different concentrations of AA with 5.0 μM DA and UA. The peak current increases proportionally to the concentration of AA (30–2000 μM) with a LOD of 10 μM. The inset displays the peak current I_{AA} (μA) against AA concentration C_{AA} (μM) and

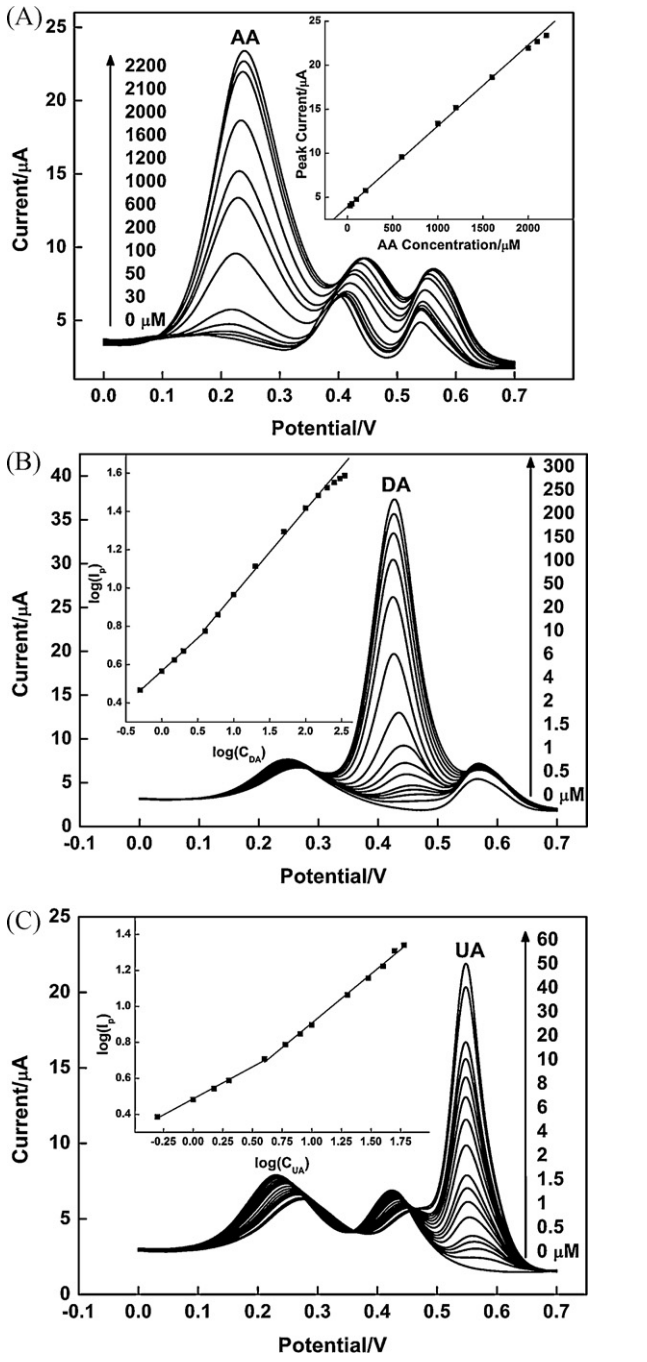

Fig. 4. SWVs of AA, DA and UA at AuNPs–β-CD–Gra/GCE in 0.10 M NaH_2PO_4–HCl buffer solution (pH 2.0): (A) 0.0–2200 μM AA in the presence of 5.0 μM DA and UA. The inset displays the plot of peak current of AA against concentration of AA. (B) 0.0–300 μM DA in the presence of 500 μM AA and 5.0 μM UA. The inset depicts the plot of logarithm of DA peak current against logarithm of DA concentration. (C) 0.0–60 μM UA in the presence of 500 μM AA and 5.0 μM DA. The inset shows the plot of logarithm of UA peak current against logarithm of UA concentration. The optimal SWV conditions are used.

the linear regression equation is: $I_{AA} = 0.00921\, C_{AA} + 3.91$ ($r = 0.999$). Fig. 4B displays the SWVs of different concentrations (0.0–300 μM) of DA with 500 μM AA and 5.0 μM UA. The peak current does not increase proportionally with the concentration of DA. Instead, the logarithm of DA peak current against logarithm of DA concentration is linearly related as shown in the inset of Fig. 4B. It has been reported that this logarithm relationship is mainly attributed to the formation of the so-called microscopic phases upon the interaction of an electron with the deposited metal on

Table 1
Comparison of analytical performance of AuNPs–β-CD–Gra/GCE with other modified electrodes in the literature.

Electrode	L-Ascorbic acid (μM)		Dopamine (μM)		Uric acid (μM)		Ref.
	Linearity	LOD	Linearity	LOD	Linearity	LOD	
AuNPs/GCE	8–5500	3	–	–	0.6–850	0.6	[33]
PPy-TDS/Au	1–500	0.4	1–500	0.4	1–500	0.6	[34]
AuNPs-PPy_{ox}/GCE	–	–	–	–	0.050–0.28	0.03	[43]
OT-HDT/Au	300–1400	90	200–1200	90	–	–	[44]
Chitosan-Gra/GCE	50–1200	50	1.0–24	1.0	2.0–45	2.0	[53]
L-Cys–AuNPs/GCE	2–800	–	–	–	2–1000	–	[62]
AuNPs–β-CD–Gra/GCE	30–2000	10	0.50–150	0.15	0.5–60	0.21	This work

Table 2
Determination and recovery test of L-ascorbic acid (AA), dopamine (DA) and uric acid (UA) in urine samples.

Urine samples	Analyte	Detected (μM)	R.S.D[a] (%)	Added (μM)	Found (μM)	R.S.D[a] (%)	Recovery (%)
	AA	ND[b]	–	500	504	0.8	101
1	DA	ND	–	10	10.6	0.6	106
	UA	0.82	2.8	10	11.1	1.9	103
	AA	ND	–	500	542	1.0	108
2	DA	ND	–	10	10.9	1.7	109
	UA	0.99	1.2	10	11.3	1.8	103
	AA	ND	–	500	514	0.4	103
3	DA	ND	–	10	9.8	2.0	98.0
	UA	0.89	4.1	10	10.6	0.6	97.1

[a]Three repeat samples are determined.
[b]ND: not detected.

the electrode, or by a decrease in reversibility of the electrode reaction at small amounts of deposit [60,61]. The curve follows in two linear segments at 0.50–4.0 μM ($\log I_{DA} = 0.342 \log C_{DA} + 0.568$; $r = 0.999$; LOD = 0.15 μM ($S/N = 3$)) and 4.0–150 μM ($\log I_{DA} = 0.453 \log C_{DA} + 0.511$; $r = 0.999$; LOD = 4.0 μM ($S/N = 3$)), where I_{DA} is the DA peak current (μA).

Fig. 4C displays the SWVs of different concentrations (0.0–60 μM) of UA with 500 μM AA and 5.0 μM DA. Again, the peak current does not increase proportionally with UA concentration rather a linear logarithm relationship is found as shown in the inset of Fig. 4C. The curve follows in two segments at 0.50–4.0 μM ($\log I_{UA} = 0.355 \log C_{UA} + 0.486$; $r = 0.999$; LOD = 0.21 μM ($S/N = 3$)) and 4.0–60 μM ($\log I_{UA} = 0.545 \log C_{UA} + 0.362$; $r = 0.999$; LOD = 0.21 μM ($S/N = 3$)), where I_{UA} is the UA peak current (μA) and C_{UA} is the UA concentration.

Table 1 summarizes the analytical performances of our proposed AuNPs–β-CD–Gra/GCE and the literature methods in terms of linearity and LOD. Our method has the lowest LOD for DA whereas the linearity working ranges for AA, DA and UA are comparable to the literature methods. These results demonstrate that the AuNPs–β-CD–Gra/GCE method could be an alternative choice for determining AA, DA and UA.

Real samples analysis

Since the AuNPs–β-CD–Gra/GCE possesses good sensitivity and selectivity for the simultaneous determination of AA, DA and UA, it was applied to analyze the UA content in human urine. Fig. 5 depicts the SWVs of 0.10 M NaH_2PO_4–HCl buffer solution (pH 2.0) in the absence and presence of human urine sample using the optimal SWV conditions. A large increase in peak current at 0.546 V is obtained, indicating that UA is in the urine sample.

Table 2 summarizes the analysis and recovery test of AA, DA and UA in human urine samples by using the AuNPs–β-CD–Gra/GCE. All the samples do not require pretreatment and can be analyzed directly. The results show that our proposed method is simple, convenient and reliable for simultaneous determination of AA, DA and UA in urine.

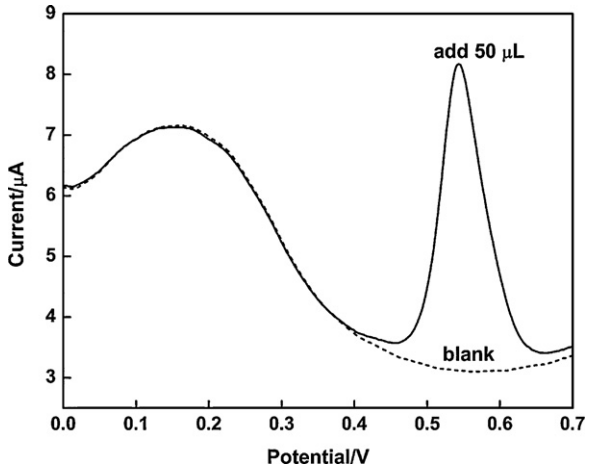

Fig. 5. Typical SWVs at AuNPs–β-CD–Gra/GCE in 25 mL 0.10 M NaH_2PO_4–HCl buffer solution (pH 2.0) in the absence and presence of 50 μL human urine.

Conclusion

A novel modified glassy carbon electrode has been successfully fabricated by using graphene decorated with gold nanoparticles. The AuNPs–β-CD–Gra/GCE exhibits good electro-activity to the oxidation of AA, DA and UA. The oxidation peaks are well separated by applying SWV. The detection limit of DA and UA are 0.15 and 0.21 μM, respectively. The AuNPs–β-CD–Gra/GCE provides good stability, sensitivity and selectivity to determine DA and UA in the presence of AA. The sensitivity of AuNPs–β-CD–Gra nanocomposite could be significantly enhanced by AuNPs, possibly attributing to the increase in electric conductivity and the effective surface area of AuNPs. The proposed method is a promising tool for simultaneous determination of AA, DA and UA in urine. It is anticipated that further surface modification of Gra with other metal NPs could be promising strategy for developing other highly efficient and selective electrochemical sensors. Further work is being conducted and the results will be published in due course.

Acknowledgments

Financial supports from the Specialized Research Fund for Instrument Program of National Natural Science Foundation of China (20927007), National Natural Science Foundation of China (21175094 and 20803050) and the Open Foundation Project of State Key Laboratory of Electronic Thin Films and Integrated Devices of University of Electronic Science and Technology of China (KFJJ200918) are gratefully acknowledged.

Appendix A. Supplementary data

Supplementary data associated with this article can be found, in the online version, at doi:10.1016/j.talanta.2012.01.047.

References

[1] A.N. Shipway, E. Katz, I. Willner, ChemPhysChem 1 (2000) 18–52.
[2] C.M. Cobley, J.Y. Chen, E.C. Cho, L.V. Wang, Y.N. Xia, Chem. Soc. Rev. 40 (2011) 44–56.
[3] R.D. Powell, J.F. Hainfeld, Micron 42 (2011) 163–174.
[4] N. Uehara, Anal. Sci. 26 (2010) 1219–1228.
[5] J. Tashkhourian, M.R.H. Nezhad, J. Khodavesi, S. Javadi, J. Electroanal. Chem. 633 (2009) 85–91.
[6] W.N. Hu, D.M. Sun, W. Ma, Electroanalysis 22 (2010) 584–589.
[7] U. Yogeswaran, S. Thiagarajan, S.M. Chen, Anal. Biochem. 365 (2007) 122–131.
[8] S. Thiagarajan, S.M. Chen, Talanta 74 (2007) 212–222.
[9] J.S. Huang, Y. Liu, H.Q. Hou, T.Y. You, Biosens. Bioelectron. 24 (2008) 632–637.
[10] C. Deeb, X.A. Zhou, D. Gerard, A. Bouhelier, P.K. Jain, J. Plain, O. Soppera, P. Royer, R. Bachelott, J. Phys. Chem. Lett. 2 (2011) 7–11.
[11] A.S. Stender, G.F. Wang, W. Sun, N. Fang, ACS Nano 4 (2010) 7667–7675.
[12] S.J. Guo, E.K. Wang, Anal. Chim. Acta 598 (2007) 181–192.
[13] V. Serafin, M. Eguilaz, L. Agui, P. Yanez-Sedeno, J.M. Pingarron, Electroanalysis 23 (2011) 169–176.
[14] J.M. Pingarron, P. Yanez-Sedeno, A. Gonzalez-Cortes, Electrochim. Acta 53 (2008) 5848–5866.
[15] N. Reum, C. Fink-Straube, T. Klein, R.W. Hartmann, C.M. Lehr, M. Schneider, Langmuir 27 (2011) 861.
[16] S.H. Lim, J. Wei, J.Y. Lin, Chem. Phys. Lett. 400 (2004) 578–582.
[17] R.Y. Zhang, X.M. Wang, Chem. Mater. 19 (2007) 976–978.
[18] H.J. Jiang, Y. Zhao, H. Yang, D.L. Akins, Mater. Chem. Phys. 114 (2009) 879–883.
[19] A.P. Tuan, B.C. Choi, K.T. Lim, Y.T. Jeong, Appl. Surf. Sci. 257 (2011) 3350–3357.
[20] Y.J. Hu, J.A. Jin, P. Wu, H. Zhang, C.X. Cai, Electrochim. Acta 56 (2010) 491–500.
[21] B. Li, G. Lu, X.Z. Zhou, X.H. Cao, F. Boey, H. Zhang, Langmuir 25 (2009) 10455–10458.
[22] S. Malola, H. Hakkinen, P. Koskinen, Appl. Phys. Lett. 94 (2009) 043106.
[23] S. Mao, G.H. Lu, K.H. Yu, Z. Bo, J.H. Chen, Adv. Mater. 22 (2010) 3521–3526.
[24] R. Muszynski, B. Seger, P.V. Kamat, J. Phys. Chem. C 112 (2008) 5263–5266.
[25] X.Q. Fu, F.L. Bei, X. Wang, S. O'Brien, J.R. Lombardi, Nanoscale 2 (2010) 1461–1466.
[26] W.J. Hong, H. Bai, Y.X. Xu, Z.Y. Yao, Z.Z. Gu, G.Q. Shi, J. Phys. Chem. C 114 (2010) 1822–1826.
[27] F. Liu, J.Y. Choi, T.S. Seo, Chem. Commun. 46 (2010) 2844–2846.
[28] K.F. Zhou, Y.H. Zhu, X.L. Yang, J. Luo, C.Z. Li, S.R. Luan, Electrochim. Acta 55 (2010) 3055–3060.
[29] F.A. He, J.T. Fan, F. Song, L.M. Zhang, H.L.W. Chan, Nanoscale 3 (2011) 1182–1188.
[30] M.H. Yang, B.G. Choi, H. Park, T.J. Park, W.H. Hong, S.Y. Lee, Electroanalysis 23 (2011) 850–857.
[31] C.B. Liu, K. Wang, S.L. Luo, Y.H. Tang, L.Y. Chen, Small 7 (2011) 1203–1206.
[32] S.J. Padayatty, A. Katz, Y.H. Wang, P. Eck, O. Kwon, J.H. Lee, S.L. Chen, C. Corpe, A. Dutta, S.K. Dutta, M. Levine, J. Am. Coll. Nutr. 22 (2003) 18–35.
[33] G.Z. Hu, Y.G. Ma, Y. Guo, S.J. Shao, Electrochim. Acta 53 (2008) 6610–6615.
[34] Z.Q. Gao, H. Huang, Chem. Commun. (1998) 2107–2108.
[35] T. Selvaraju, R. Ramaraj, J. Appl. Electrochem. 33 (2003) 759–762.
[36] Y.H. Zhang, S. Su, Y. Pan, L.P. Zhang, Y.J. Cai, Ann. Chim. (Rome) 97 (2007) 665–674.
[37] A.A. Ensafi, M. Taei, T. Khayamian, J. Electroanal. Chem. 633 (2009) 212–220.
[38] X.H. Zhu, X.Q. Lin, Chin. J. Chem. 27 (2009) 1103–1109.
[39] M. Pandurangachar, B.E.K. Swamy, U. Chandra, O. Gilbert, B.S. Sherigara, Int. J. Electrochem. Sci. 4 (2009) 672–683.
[40] H. Yao, Y.Y. Sun, X.H. Lin, Y.H. Tang, L.Y. Huang, Electrochim. Acta 52 (2007) 6165–6171.
[41] R. Manjunatha, G.S. Suresh, J.S. Melo, S.F. D'Souza, T.V. Venkatesha, Sens. Actuators B 145 (2010) 643–650.
[42] S.R. Jeyalakshmi, S.S. Kumar, J. Mathiyarasu, K.L.N. Phani, V. Yegnaraman, Indian J. Chem. A 46 (2007) 957–961.
[43] J. Li, X.Q. Lin, Anal. Chim. Acta 596 (2007) 222–230.
[44] J.B. Raoof, A. Kiani, R. Ojani, R. Valiollahi, S. Rashid-Nadimi, J. Solid State Electrochem. 14 (2010) 1171–1176.
[45] M. Noroozifar, M. Khorasani-Motlagh, A. Taheri, Talanta 80 (2010) 1657–1664.
[46] P. Shakkthivel, S.M. Chen, Biosens. Bioelectron. 22 (2007) 1680–1687.
[47] S. Thiagarajan, T.H. Tsai, S.M. Chen, Biosens. Bioelectron. 24 (2009) 2712–2715.
[48] Y. Liu, J.S. Huang, H.Q. Hou, T.Y. You, Electrochem. Commun. 10 (2008) 1431–1434.
[49] Z. Dursun, B. Gelmez, Electroanalysis 22 (2010) 1106–1114.
[50] Safavi, N. Maleki, O. Moradlou, F. Tajabadi, Anal. Biochem. 359 (2006) 224–229.
[51] D. Zheng, J.S. Ye, L. Zhou, Y. Zhang, C.Z. Yu, J. Electroanal. Chem. 625 (2009) 82–87.
[52] S.Y. Zhu, H.J. Li, W.X. Niu, G.B. Xu, Biosens. Bioelectron. 25 (2009) 940–943.
[53] D.X. Han, T.T. Han, C.S. Shan, A. Ivaska, L. Niu, Electroanalysis 22 (2010) 2001–2008.
[54] H.R. Zare, N. Nasirizadeh, M.M. Ardakani, J. Electroanal. Chem. 577 (2005) 25–33.
[55] X.B. Fan, W.C. Peng, Y. Li, X.Y. Li, S.L. Wang, G.L. Zhang, F.B. Zhang, Adv. Mater. 20 (2008) 4490–4493.
[56] S. Pande, S.K. Ghosh, S. Praharaj, S. Panigrahi, S. Basu, S. Jana, A. Pal, T. Tsukuda, T. Pal, J. Phys. Chem. C 111 (2007) 10806–10813.
[57] G. Goncalves, P.A.A.P. Marques, C.M. Granadeiro, H.I.S. Nogueira, M.K. Singh, J. Gracio, Chem. Mater. 21 (2009) 4796–4802.
[58] R.S. Nicholson, I. Shain, Anal. Chem. 36 (1964) 706–723.
[59] Y.F. Zhao, Y.Q. Gao, D.P. Zhan, H. Liu, Q. Zhao, Y. Kou, Y.H. Shao, M.X. Li, Q.K. Zhuang, Z.W. Zhu, Talanta 66 (2005) 51–57.
[60] S.A. Kozina, J. Anal. Chem. 58 (2003) 954–958.
[61] G.-J. Lee, H.M. Lee, Y.R. Uhm, M.K. Lee, C.-K. Rhee, Electrochem. Commun. 10 (2008) 1920–1923.
[62] Y. Cui, C. Yang, W. Pu, M. Oyama, J. Zhang, Anal. Lett. 43 (2009) 22–33.